# Joint Uptake and Body Distribution of a Technetium-99m-Labeled Anti-Rat-CD4 Monoclonal Antibody in Rat Adjuvant Arthritis

Raimund W. Kinne, Wolfgang Becker, Gerhard Simon, Giovanni Paganelli, Ernesta Palombo-Kinne, Adrian Wolski, Stefan Bloch, Alexander Schwarz, Friedrich Wolf and Frank Emmrich

*Max-Planck-Society, Clinical Research Unit for Rheumatology/Immunology, Institute of Clinical Immunology; Department of Nuclear Medicine, University of Erlangen-Nuremberg, Erlangen, FRG; Radiochemical Laboratory of the Behring Werke (Hoechst AG), Frankfurt, FRG; and Department of Nuclear Medicine, Ospedale S. Raffaele, Milano, Italy*

Joint uptake and body distribution of a $^{99m}$Tc-labeled monoclonal antibody (Mab) to the rat CD4 molecule (W3/25; $IgG_1$) were investigated after intravenous injection in normal rats and in animals with experimentally induced adjuvant arthritis. An isotype-matched Mab with irrelevant specificity (anti-human carcino-embryonic-antigen) was used as control. A 4 hr sequential gamma-camera imaging revealed that both anti-CD4 and control Mab accumulated to a higher degree in arthritic than in normal ankle joints; the accumulation was comparable for the two Mabs. In contrast to the inflamed joints, a specific accumulation of the anti-CD4 Mab was found in organs rich in CD4-positive cells, i.e. spleen, bone marrow and lymph nodes, as assessed by direct well counter measurements 16 hr after injection. The control Mab displayed no preferential organ accumulation in either normal or diseased animals. These results indicate that a specific accumulation of anti-CD4 Mabs occurs in CD4-positive-cell-rich tissues in both normal and diseased animals and that immunoglobulins accumulate preferentially in inflamed joints regardless of their antibody specificity.

**J Nucl Med 1993; 34:92–98**

Human rheumatoid arthritis (RA) is characterized by a severe chronic synovitis, in which CD4-positive T-cells, the helper/inducer subset of T lymphocytes, are likely to play a predominant role (*1–3*). Recent studies have shown a beneficial effect of anti-CD4 monoclonal antibodies (Mabs) in the treatment of RA (*4,5*). In one of these studies the therapeutically applied Mab was radiolabeled and used to image inflamed joints (*6*). However, given the obvious limitations of studies in humans, it could not be clarified whether the immunological specificity of the anti-CD4 Mab determined its accumulation or whether immunoglobulins accumulate nonspecifically in the arthritic joint.

Experimentally induced rat adjuvant arthritis (AA) shows many similarities to human RA (*7–9*) and was therefore chosen to investigate whether the accumulation of an anti-CD4 Mab differed from that of an isotype-matched Mab (anti-human carcinoembryonic-antigen; CEA) used as control.

## MATERIALS AND METHODS

### Animals

Female Lewis rats (140–220 g, age 7–18 wk, Charles River Laboratories, Sulzfeld, FRG) were injected intradermally into the tail base with 0.1 ml of a solution containing 2.5 mg of heat-killed mycobacterium tuberculosis (MT, R37 Ra; Difco, Detroit, MI) per ml in paraffin oil (Riedel de Haën AG, Seelze, FRG). Arthritic lesions of the four paws were graded from 0–4 according to the extent of erythema and edema of the periarticular tissue; 16 was the maximum score per animal (*10*). Only animals with a minimum score of 2.5 in the inflamed ankle joint were used to obtain pinhole images. Arthritis began to develop in the rats 10–13 days after injection of MT; peaked at day 18–24; and declined thereafter (*11,12*). For the present study, rats were used at day 19 after injection of MT along with age and gender matched normal control animals. The rats were assigned to four different groups; normal rats receiving anti-CEA Mabs (total: n = 7), or anti-CD4 Mabs (n = 11), as well as arthritic rats receiving anti-CEA Mabs (n = 9), or anti-CD4 Mabs (n = 10). Dissections, pinhole scans and whole-body scans were not necessarily performed on all animals in the initial groups, due to a number of technical reasons not related to the arthritic status of the animals.

On the day of the experiment, rats were anesthetized with diethyl-ether (Merck, Darmstadt, FRG); a 7-cm long polyethylene catheter (Bardi-Kath, Bard Limited, Sunderland, UK) was inserted into the right common jugular vein to allow central venous application of the Mabs. The opposite end of the catheter, covered with a rubber head, was subcutaneously led to emerge from the dorsal neck and sutured below the interauricular line (*13*). To allow arterial blood sampling, a similar procedure was applied in a separate group of arthritic animals (n = 3) to catheterize the right carotid artery.

Received Mar. 4, 1992; revision accepted Aug. 6, 1992.

For reprints or correspondence contact: Raimund W. Kinne, MD, Max-Planck-Society, Clinical Research Unit for Rheumatology/Immunology, Schwabachanlage 10, D-8520 Erlangen, FRG.

### Antibodies

The anti-rat-CD4 Mab (W3/25, $IgG_1$; European Collection of Animal Cell Cultures, ECACC, Salisbury, UK) is directed against the equivalent of the human CD4 molecule on rat T-helper lymphocytes and macrophages (*14–16*). The affinity of this anti-CD4 Mab for the CD4 molecule can be calculated as $\geq 3 \times 10^{-9}$ $M^{-1}$ on the basis of its association and dissociation constants (*17*; Mason DW, *personal communication*).

The anti-human-CEA Mab BW 431/26 ($IgG_1$; Behring Werke, Frankfurt, FRG) reacts with the carcinoembryonic-antigen on the majority of colon carcinomas (*18*). This Mab was chosen as control because it did not show a positive reaction on cryostat sections of either normal or inflamed rat synovial membrane, nor of rat large intestine, applying immunohistochemical techniques (Kinne RW, unpublished results).

### Radiolabeling of the Antibodies

Mabs were radiolabeled according to the mercaptoethanol method of Schwarz and Steinsträsser (*19*). They were provided as a kit with 1 mg (anti-rat-CD4 Mab) or 2 mg (anti-human-CEA Mab) of the lyophilized, partially reduced antibody together with a Sn (II)-complex. One mg of either Mab was incubated with 120–200 MBq of $^{99m}Tc$. The injectant contained less than 1% free pertechnetate 10 min and 3 hr after radiolabeling as measured by high-performance liquid chromatography (Schwarz A, *personal communication*).

### Intravenous Injection and Imaging

After the rats had recovered from catheterization for at least 2 hr, they were anesthetized by intramuscular injection of urethane (0.75 g/kg body weight; Sigma, Deisenhofen, FRG) and immobilized on a stretcher under a gamma-camera. Two hundred micrograms (16–38 MBq) of $^{99m}Tc$-labeled Mabs were then slowly injected through the central venous catheter. The accumulation of radiolabeled Mabs in the ankle joint was followed in 20-min frames for the first 4 hr using a Siemens Basicam gamma camera equipped with a pinhole collimator (Siemens, Erlangen, FRG) and interfaced to a computer system (DEC-gammaM, Digital Equipment, Nuremberg, FRG). Integrated radioactivity distribution was measured on a 64 × 64 matrix.

Fifteen hours after injection of the Mabs, a whole body scan of the rats was acquired using the same imaging parameters. For these scans the gamma-camera was fitted with a high-resolution, low-energy collimator.

### Biodistribution of Mabs

Sixteen hours after injection, organs, tissues and joints listed in Table 1 were excised. Blood (~7–8 ml) was withdrawn through the central venous catheter. The feces were obtained from the distal ileum. The bone marrow contained in both distal femur and proximal tibia was flushed out with saline, the suspension was then centrifuged and supernatant and pellet separated. The resulting pellet was weighed. For determination of the radioactivity contained in the bone marrow, the supernatant was added back to the pellet. Skin was removed from the hip at the level of the crista iliaca. A sample of muscle tissue was obtained from the musculus quadriceps femoris. The radioactivity contained in the different preparations was then counted in a well gamma-counter. Values were expressed as a percentage of the total body activity, and per grams of wet weight of the samples. Alternatively, for the comparison of whole-body scans at 15 hr after injection and well counter measurements at 16 hr after injection, values for the joint radioactivity were expressed as a percentage of total body activity.

### Immunohistological Detection of Biotinylated Anti-CD4 Mab in Lymphoid Organs

Biotinylated anti-CD4 Mab was detected in cryostat sections of lymphoid organs from AA rats 24 hr after intravenous injection (2 mg W3/25) using the alkaline phosphatase technique. Cryostat sections were cut, air-dried and fixed for 10 min each in ice-cold acetone and chloroform (Merck, Darmstadt, FRG). Streptavidine-alkaline phosphatase (Dakopatts, Hamburg, FRG) was added at a concentration of 1:100 for 1 hr. The alkaline phosphatase was developed in a solution of 125 mg naphtol AS-BI phosphate (Sigma, Deisenhofen, FRG) in 1.5 ml dimethylformamide (Merck, Darmstadt, FRG), 175 ml of 0.01 *M* TBS-buffer and 62.5 ml of 0.2 *M* propandiol-buffer (both Merck, Darmstadt, FRG) containing 100 mg levamisole (Sigma, Deisenhofen, FRG; final pH 8.8); 25 mg Neufuchsin (Merck, Darmstadt, FRG) in 500 µl 2 N HCL were mixed with 50 mg Na-nitrite (Merck, Darmstadt, FRG) in 1250 µl of distilled water; Neufuchsin was added and the solution was filtered. Sections were counterstained with Mayer's hematoxylin.

### Scan Evaluation

Pinhole images of arthritic and normal recipient rats were evaluated using the region of interest (ROI) technique. A 36-pixel ROI was placed over the ankle joint. A reference region of equal size was placed over the distal lower leg. The results were expressed as counts accumulated in the two regions during time frames of 20 min, corrected for the decay of $^{99m}Tc$. Alternatively, the data were expressed as the ratio between the radioactivity levels in the ankle joint region and those in the reference region. In addition, the radioactivity accumulated in ankle and wrist joints 15 hr after injection of the Mabs was determined by placing regions over the joints in whole-body scans. Values were expressed as the ratio between the counts in these regions and the whole-body counts in percentages.

### Plasma Clearance of $^{99m}Tc$-Labeled Mabs

Timed arterial blood samples (approx. 100 µl) were collected from the rats (n = 3) into a heparinized tube or syringe. An aliquot of 50 µl blood was transferred into an Eppendorf tube and centrifuged. The radioactivity contained in plasma (30 µl) and blood cells was then separately measured in a well-counter. Arterial blood samples were taken three times during first minute, then every minute for the first 5 min, every 5 min for the first hour, every 15 min for the second hour and every 30 min for the third and fourth hours.

### Statistics

A nonparametric test (Kruskall-Wallis Test) was used to compare the radioactivity values of the two different Mabs in tissue preparations. Due to the high number of comparisons, significance in this test was accepted at a level of $p \leq 0.005$. Organs and tissues showing significant differences in the Kruskall-Wallis-Test were then analyzed for differences among groups by the Mann-Whitney (U) test, with significant differences accepted at $p \leq 0.01$. For both ROI evaluations of whole-body scans and direct tissue determination of joint radioactivity as a percentage of the total body activity, the Mann-Whitney (U) test was applied; statistical significance was accepted at $p \leq 0.05$. Radioactivity

**TABLE 1**
Distribution of Anti-Human-CEA and Anti-Rat-CD4 Mabs in Normal and Arthritic Recipient Rats

| Tissues | Normal recipients | | Arthritic recipients | |
|---|---|---|---|---|
| | anti-CEA (n = 6) | anti-CD4 (n = 8) | anti-CEA (n = 6) | anti-CD4 (n = 6) |
| Thymus | 1.0 ± 0.1 | 0.7 ± 0.1 | 1.6 ± 0.2 | 0.7 ± 0.1 |
| Lungs | 3.5 ± 0.4 | 1.3 ± 0.2 | 2.4 ± 0.3 | 1.9 ± 0.7 |
| Liver | 2.0 ± 0.2 | 8.6 ± 0.7§ | 2.2 ± 0.1 | 7.7 ± 0.3§ |
| Spleen | 1.7 ± 0.2 | 19.1 ± 1.1§ | 2.4 ± 0.3 | 16.8 ± 1.1§ |
| Intestine (small) | 2.0 ± 0.2 | 1.9 ± 0.3 | 2.0 ± 0.5 | 1.4 ± 0.1 |
| Intestine (large) | 1.0 ± 0.3 | 1.6 ± 0.3 | 0.8 ± 0.3 | 0.6 ± 0.2 |
| Feces | 3.2 ± 1.0 | 1.0 ± 0.4 | 1.2 ± 0.5 | 1.3 ± 0.7 |
| Kidneys | 8.6 ± 1.1 | 9.1 ± 0.3 | 5.9 ± 0.7 | 8.3 ± 1.1 |
| Blood (whole) | 6.1 ± 0.4 | 0.5 ± 0.1§ | 6.1 ± 0.6 | 0.6 ± 0.2§ |
| Blood cells | 1.2 ± 0.2 | 0.3 ± 0.0§ | 1.5 ± 0.2 | 0.3 ± 0.1‡ |
| Plasma | 7.6 ± 1.1 | 1.1 ± 0.3§ | 7.0 ± 0.7 | 1.0 ± 0.3‡ |
| Bone marrow | 1.5 ± 0.2 | 2.3 ± 0.4 | 0.7 ± 0.1 | 2.5 ± 0.1§ |
| Peyer's plaques | 1.2 ± 0.1 | 2.3 ± 0.5 | 1.5 ± 0.2 | 2.1 ± 0.3 |
| Mesenteric ln. | 1.2 ± 0.2 | 6.6 ± 1.1§ | 1.8 ± 0.3 | 4.8 ± 0.2§ |
| Submandibular ln. | 1.1 ± 0.1 | 3.7 ± 1.3 | 1.1 ± 0.1 | 1.9 ± 0.3 |
| Axillar ln. | 0.6 ± 0.1 | 1.8 ± 0.4 | 0.8 ± 0.1 | 1.1 ± 0.2 |
| Subscapular ln. | 0.4 ± 0.1 | 2.0 ± 0.4§ | 0.7 ± 0.2 | 1.2 ± 0.3 |
| Inguinal ln. | 1.0 ± 0.2 | 1.8 ± 0.4 | 0.6 ± 0.1 | 0.9 ± 0.2 |
| Popliteal ln. | 0.5 ± 0.1 | 2.6 ± 0.6 | 0.7 ± 0.1 | 1.1 ± 0.2 |
| Retroperitoneal ln. | 1.2 ± 0.2 | 2.8 ± 0.7 | 1.0 ± 0.2 | 1.5 ± 0.3 |
| Toes | 0.4 ± 0.1 | 0.2 ± 0.0 | 0.5 ± 0.1 | 0.3 ± 0.0 |
| Ankles | 0.5 ± 0.1 | 0.3 ± 0.0 | 2.8 ± 0.2† | 1.6 ± 0.2†‡ |
| Knees | 1.3 ± 0.2 | 2.1 ± 0.2 | 1.7 ± 0.2 | 2.4 ± 0.3 |
| Fingers | 0.3 ± 0.0 | 0.2 ± 0.0 | 0.7 ± 0.2 | 0.4 ± 0.1 |
| Wrists | 0.4 ± 0.1 | 0.3 ± 0.1 | 1.0 ± 0.2 | 0.6 ± 0.1 |
| Elbows | 0.3 ± 0.0 | 0.4 ± 0.1 | 0.5 ± 0.1 | 0.3 ± 0.0 |
| Skin | 0.4 ± 0.2 | 0.2 ± 0.0 | 0.2 ± 0.0 | 0.1 ± 0.0 |
| Muscle | 0.2 ± 0.0 | 0.1 ± 0.0 | 0.4 ± 0.2 | 0.1 ± 0.0 |
| Synovia | | | 2.2 ± 0.4 | 1.4 ± 0.4 |

Mean ± s.e.m. of % total body radioactivity per grams of sample wet weight. Values for the left and right side of bilateral tissues or organs were added. ln. = lymph nodes.

* $p \leq 0.01$.

† $p \leq 0.005$ Mann-Whitney U-test for the comparison between normal and arthritic recipients.

‡ $p \leq 0.01$.

§ $p \leq 0.005$ Mann-Whitney U-test for the comparison between anti-CD4 and anti-CEA Mabs.

levels obtained by ROI evaluations of pinhole scans (see Fig. 4) were tested for differences between the two Mabs by comparing the areas under the curve employing the Mann-Whitney (U) test (statistical significance at $p \leq 0.05$).

## RESULTS

### Clinical Scores of the Rats With AA

The clinical score of arthritic animals receiving the anti-CD4 Mab (n = 10) varied between 1.5 and 4 [mean 3.3 ± 0.2 (s.e.m.)] for the hindpaws, and between 0 and 4 [mean 2.4 ± 0.4 (s.e.m.)] for the forepaws. Arthritic rats injected with anti-CEA Mab (n = 9) showed a mean score of 3.2 ± 0.3 (s.e.m.) for the hindpaws, and 1.6 ± 0.3 (s.e.m.) for the forepaws. Normal control animals showed no signs of inflammation in fore- or hindpaws.

### Plasma Clearance of Mabs

Maximal arterial plasma concentration of both anti-CD4 and anti-CEA Mabs was reached within 40 sec after intravenous bolus injection (Fig. 1). Plasma levels of the anti-CEA remained slightly higher compared to the anti-CD4 Mab, but no significant differences were observed throughout the 4 hr experimental period.

### Pinhole Gamma Camera Scanning of Ankle Joints

*Anti-CD4 Mab.* In gamma-camera images obtained 4 hr after intravenous injection, the anti-CD4 Mab accumulated to a greater extent in arthritic joints (Fig. 2B) in comparison to ankle joints of normal animals (Fig. 2D). The radioactivity in the arthritic ankle joint continued to increase until 4 hr after injection of the labeled Mab (Fig.

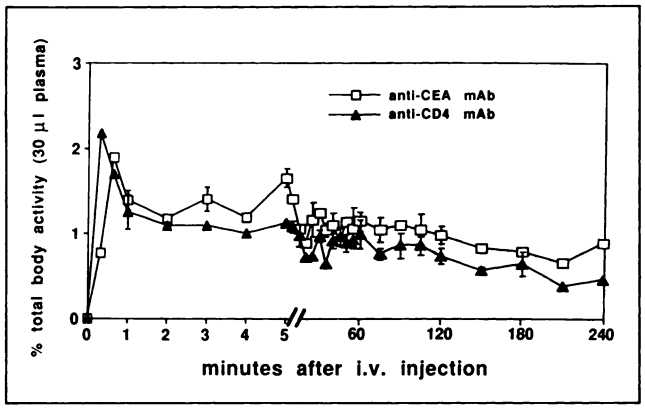


**FIGURE 1.** Arterial plasma clearance of anti-CEA (open squares) and anti-CD4 Mabs (closed triangles) throughout the initial 4 hr after intravenous injection into arthritic animals. Values shown are means ± s.e.m. (n = 3). The clearance of both Mabs from circulation is comparable.

3B). In contrast, there was no accumulation of label in the distal lower leg adjacent to the inflamed joint, chosen as reference (Fig. 3B). The uptake in the lower leg of arthritic animals having received anti-CD4 was not significantly different from that of normal animals injected with either one of the Mabs (Fig. 3C, D).

*Anti-Human CEA Mab.* The control Mab (Fig. 2A) accumulated in arthritic joints in a fashion indistinguishable from the anti-CD4 Mab (Fig. 2B). As for the anti-CD4 Mab, increasing levels of radioactivity in the arthritic ankle joint in contrast to steady levels in the lower leg could be observed throughout the investigation period of 4 hr after injection (Fig. 3A).

In normal control rats, the accumulation of anti-CEA Mab in ankle joint and lower leg (Fig. 2C; 3C) was also very similar to that of the anti-CD4 Mab (Fig. 2D; 3D).

The marked similarity in the distribution of the two antibodies in ankle joints of both normal and arthritic rats was also observed when the radioactivity levels were expressed as a ratio between ankle joint and lower leg (Fig. 4).

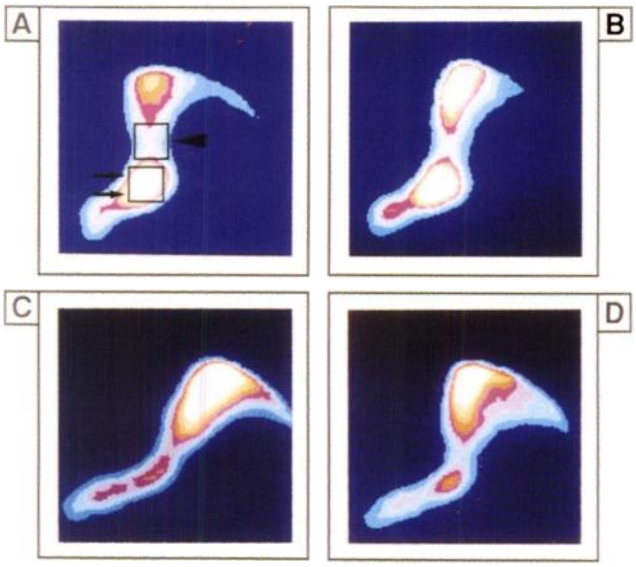


**FIGURE 2.** Gamma-camera images of ankle joint (arrows) and lower leg (arrowhead) of arthritic (A,B) and normal (C,D) rats 4 hr after intravenous injection of radiolabeled anti-CEA Mab (A,C) or anti-CD4 Mab (B,D). Colors represent levels of radioactivity ranging from low (blue) to high (white). Arthritic joints (A,B) show higher radioactivity levels than normal joints (C,D). There appears to be no difference between the two Mabs used.

### Whole Body Gamma Camera Scanning

*Anti-CD4 Mab.* Fifteen hours after intravenous injection of the anti-CD4 Mab, a total of 2.4% ± 0.3% (mean ± s.e.m.) of the total body radioactivity had accumulated in arthritic ankle and wrist joints, compared to 0.9% ± 0.1% in joints of normal animals. A comparable accumulation of the anti-CD4 Mab was demonstrated in direct tissue measurements performed 16 hr after injection of the Mabs. This resulted in total levels of 1.9% ± 0.2% (mean ± s.e.m.) of the whole body activity for arthritic ankle and wrist joints and 0.4% ± 0.0% for normal ankle and wrist joints.

*Anti-Human CEA Mab.* After intravenous injection of the control Mab, a total of 3.0% ± 0.2% (mean ± s.e.m.) of the whole-body activity was detected in arthritic ankle and wrist joints compared to 1.1% ± 0.1% in normal animals. Comparable values, i.e. 2.8% ± 0.4% (mean ± s.e.m.) for the arthritic versus 0.7% ± 0.7% for the normal ankle and wrist joints, were obtained by direct measurement of tissue radioactivity.

### Body Distribution of Mabs

*Anti-CD4 Mab.* Sixteen hours after intravenous injection, arthritic rats differed from normal animals only in the ankle joint (Table 1); this inflamed joint showed significantly higher ($p \leq 0.005$) levels of radioactivity when compared to normal ankles.

Compared to the anti-CEA Mab, the anti-CD4 Mab accumulated in organs rich in CD4-positive cells, including spleen, bone marrow and lymph nodes in both normal and arthritic animals. Such preferential accumulation also occurred in the liver.

*Anti-Human CEA Mab.* For this Mab, the ankle joint of arthritic animals was also the only site where significantly higher accumulation of radioactivity occurred in comparison to normal animals. In contrast to the body distribution of the anti-CD4 Mab, the control Mab did not show any preferential organ accumulation. Low levels of the anti-CEA Mab were found in all lymphoid organs, three of which (bone marrow, mesenteric lymph nodes, subscapular lymph nodes) attained statistical significance in comparison to the anti-CD4 Mab (Table 1).

Sixteen hours after injection, the anti-CEA Mab showed significantly higher plasma levels ($p \leq 0.01$) than the anti-CD4 Mab. At the same time, significantly higher levels

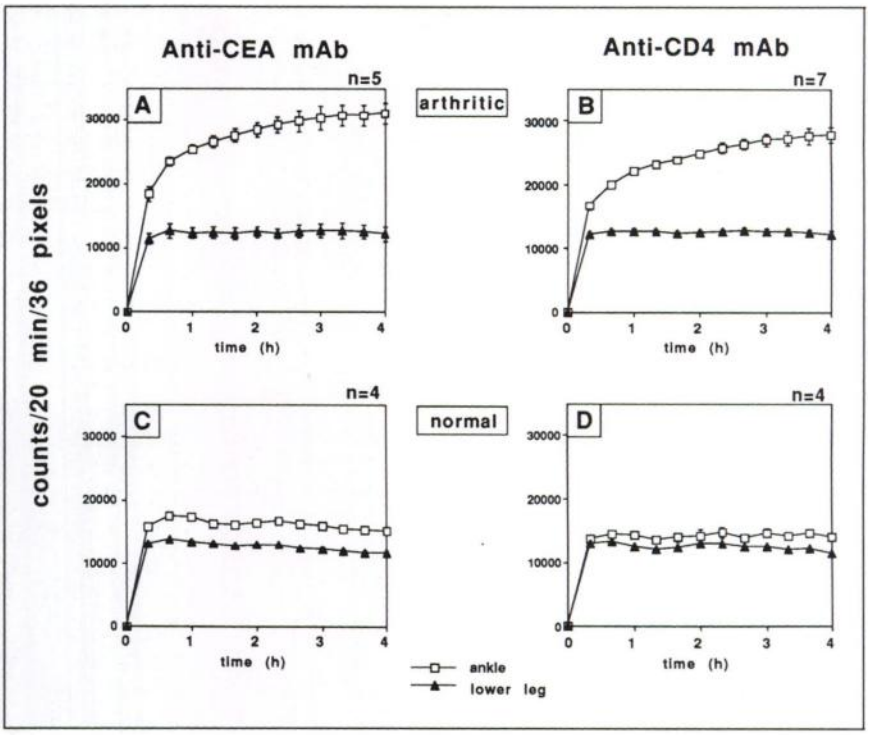


**FIGURE 3.** Joint uptake of anti-CEA Mab (A,C) and anti-CD4 Mab (B,D) in ankle joints and lower legs of arthritic (A,B) or normal (C,D) recipient rats during the first 4 hr after intravenous injection. Counts accumulated in 20 min frames in region of interest (ankle joint) and reference region (lower leg) of equal size (see Fig. 2A) are expressed as mean ± s.e.m. for the numbers of animals indicated in each graph. No obvious differences are visible in the behavior of both Mabs in either arthritic or normal animals.

($p \leq 0.01$) of anti-CEA compared to anti-CD4 Mab were found in the inflamed ankle joints.

### Immunohistological Detection of Biotinylated Anti-CD4 Mab in Lymphoid Organs

Twenty–four hours after intravenous injection, biotinylated anti-CD4 Mab was detected in a mononuclear-cell-associated pattern in a popliteal lymph node of an arthritic rat (Fig. 5). A cell-associated distribution of the anti-CD4 Mab was also observed in other lymphoid organs, i.e., spleen, Peyer's plaques and other lymph nodes (data not shown).

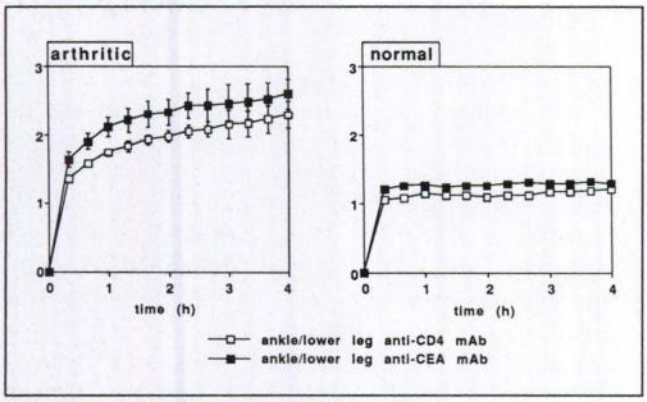


**FIGURE 4.** Joint uptake of anti-CEA (closed squares) and anti-CD4 (open squares) Mabs during the first 4 hr after intravenous injection into arthritic (left panel) and normal (right panel) rats. Values are expressed as the ratio (mean ± s.e.m.) between the counts accumulated in ankle joint and reference region in 20 min frames. There are no significant differences between the curves for the two Mabs in either arthritic or normal animals.

## DISCUSSION

The present study shows that the anti-CD4 Mab does accumulate in considerable amounts in inflamed ankle joints of rats with AA, as the radioactivity detected in the ankle joint 4 hr after injection was approximately 2.5 times higher in arthritic than in normal control rats. The presence of substantial quantities of antibody in the inflamed joint may therefore contribute to the beneficial effect of anti-CD4 treatment in AA (*9* and Milton A, *personal communication*) by local interaction of the antibody with its target at the site of inflammation, i.e. interference with antigen recognition by CD4-positive T-cells and their consecutive activation.

However, both anti-CD4 and control Mabs accumulate indistinguishably in the inflamed ankle joints of arthritic rats (Fig. 2A, B), in spite of the presence of a considerable number of CD4-positive cells as potential targets for anti-CD4 Mabs (*20*). This seems to exclude that the specificity of the anti-rat CD4 Mab per se is responsible for its increased accumulation in the inflamed joint, at least within the time frame investigated in this study. However, since the human inflamed synovial membrane contains higher numbers of CD4-positive cells than the rat synovium (*1,20*), it remains to be investigated whether imaging with anti-CD4 Mabs in human RA may provide additional benefit over nonspecific immunoglobulin.

A comparable accumulation of the two Mabs in forepaws and hindpaws of arthritic rats in whole body scans

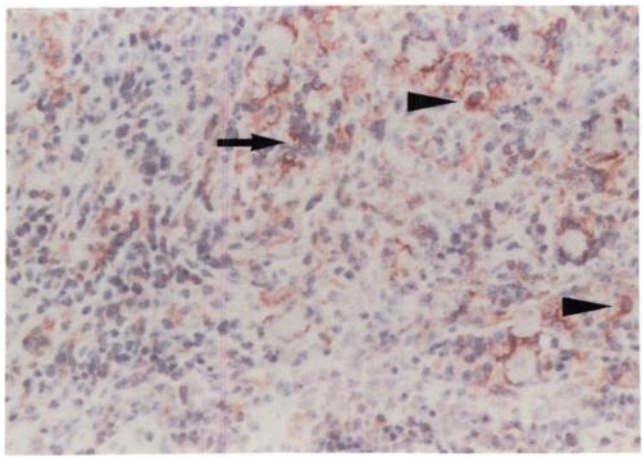

**FIGURE 5.** Immunohistological detection of biotinylated anti-CD4 Mab (red stain), 24 hr after intravenous injection, in a popliteal lymph node of a rat with adjuvant arthritis using the alkaline phosphatase technique. The antibody is associated with clusters of small cells with a low plasma-to-nucleus ratio (most likely lymphocytes; arrow) and large single cells with a high plasma-to-nucleus ratio (most likely macrophages; arrowheads). No diffuse, interstitial localization of the Mab was observed. The section was counterstained with hematoxylin. Magnification 320×.

(2.4% of the injected anti-CD4 Mab versus 3.7% of the anti-CEA Mab) shows that within 16 hr both Mabs can be used equally well for imaging purposes. A specific binding of the anti-CD4 Mab to target cells may, however, become apparent at time points later than 16 hr.

Throughout the 4 hr experimental follow-up, the anti-CEA Mab shows slightly higher plasma radioactivity levels than the anti-CD4 Mab (Fig. 1). This finding could be explained by an early and avid extraction of the anti-CD4 Mab by tissues rich in CD4-positive-cells, a phenomenon that does not occur with the anti-CEA Mab (Table 1). Because more anti-CEA Mab may therefore reach the inflamed joint, and because the tissue radioactivity detected in the inflamed joint reflects not only the interstitial but also the blood compartment, further analysis may be required to define the target-bound fraction of the anti-CD4 Mab.

The accumulation of Mabs in inflamed joints may depend on both an increased permeability of the vascular endothelium and a trapping mechanism in the arthritic joint. In inflammatory joint diseases like RA, proteins as large as or larger than IgG are found in higher concentrations in the synovial fluid in comparison to normal joints, indicating the presence of endothelial "leakage" (*21*). The increased entry of both injected Mabs in our study therefore seems to reflect a higher permeability of the inflamed endothelium for larger proteins like immunoglobulins.

It has been reported that the accumulation of immunoglobulins at sites of inflammation caused by bacterial infection depends on the presence of their Fc parts (*22, 23*). However, recent studies (*24–27*) have indicated that binding of immunoglobulins to Fc-receptors in infectious foci may be of minor if any importance for external imaging. In addition, it is not clear whether Fc receptor-mediated binding of immunoglobulin also contributes to the accumulation of such molecules in arthritic joints (*28*). However, at present, a binding of both anti-CD4 and anti-CEA mouse Mabs to high numbers of Fc-receptors present in the inflamed rat joint cannot be totally excluded.

Comparable percent values of the whole body radioactivity in arthritic joints were obtained by both whole body scans and direct tissue radioactivity measurements. These data indicate that gamma-camera scans are a suitable method to reveal the accumulation of radiolabeled Mabs in AA inflamed joints, and confirm the results of other investigators (*28*) who used Technetium-99m-labeled non-specific human IgG for the imaging of inflamed joints in rat collagen-induced arthritis.

In contrast to similar behavior in inflamed joints, anti-CD4 and anti-CEA Mabs showed clearly different body distributions (Table 1). The accumulation of anti-CD4 Mabs in lymphoid organs, such as spleen, bone marrow and lymph nodes, indicates that anti-T-cell Mabs are a highly suitable tool to specifically recognize sites with a high abundance of T-cells. This argument is supported by immunohistological detection of injected anti-CD4 Mab in lymphoid organs in a clearly cell-associated pattern (Fig. 5). Consequently, systemic therapeutic effects of anti-CD4 Mabs in lymphoid organs, in addition to possible local effects in inflamed joints, may be considered to explain the beneficial effects of treatment of both RA and AA.

The feature of anti-CD4 Mabs to specifically recognize T-cell rich areas can be usefully applied to target radiochemicals, as already demonstrated by using $^{111}$Indium-labeled pan-T-cell Mabs for the identification of cutaneous T-cell lymphoma sites (*29*), or else by the effectiveness in reducing the doses of radiotherapeutics in the treatment of non-Hodgkin's B-cell lymphoma (*30*).

The present findings may be of interest for the evaluation of imaging strategies and may also contribute basic data on anti-CD4 Mab distribution, helpful to understand the beneficial effects of anti-T-cell Mab therapy in arthritis.

## ACKNOWLEDGMENTS

The authors would like to thank U. Vorderwülbecke for expert technical assistance, Barbara Thompson for secretarial assistance and Kathleen Schmidt for her helpful suggestions. We also thank Dr. M. Meyer, Institute for Medical Statistics and Documentation, University of Erlangen-Nuremberg, for technical advice on the statistical analysis. The Max-Planck-Society Clinical Research Unit for Rheumatology/Immunology is funded by the German Ministry for Research and Technology (BMFT).

## REFERENCES

1. Burmester GR, Yu DTY, Irani AM, Kunkel HG, Winchester RJ. Ia+ T cells in synovial fluid and tissue of patients with rheumatoid arthritis. *Arthritis Rheum* 1981;24:1370–1376.
2. Janossy G, Duke O, Poulter LW, Panayi G, Bofill M, Goldstein G. Rheumatoid arthritis: a disease of T-lymphocyte/macrophage immunoreg-

ulation. *Lancet* 1981;839–842.
3. Fox DA, Millard JA, Kan L, et al. Activation pathways of synovial T lymphocytes. Expression and function of the UM4D4/CDw60 antigen. *J Clin Invest* 1990;86:1124–1136.
4. Herzog C, Walker C, Pichler W, et al. Monoclonal anti-CD4 in arthritis. *Lancet* 1987;II:1461–1462.
5. Horneff G, Burmester GR, Emmrich F, Kalden JR. Treatment of rheumatoid arthritis with an anti-CD4 monoclonal antibody. *Arthritis Rheum* 1991;34:129–140.
6. Becker W, Emmrich F, Horneff G, et al. Imaging rheumatoid arthritis specifically with technetium 99m CD4-specific (T-helper lymphocytes) antibodies. *Eur J Nucl Med* 1990;17:156–159.
7. Pearson CM, Wood FD. Studies of arthritis and other lesions induced in rats by the injection of mycobacterial adjuvant. VII. Pathologic details of the arthritis and spondylitis. *Am J Pathol* 1963;42:73–95.
8. Taurog JD, Argentieri DC, Reynolds RA. Adjuvant arthritis. *Methods Enzymol* 1988;162:339–355.
9. Billingham MEJ, Hicks C, Carney S. Monoclonal antibodies and arthritis. *Agents Actions* 1990;29:77–87.
10. Wood FD, Pearson CM, Tanaka A. Capacity of mycobacterial wax D and its subfractions to induce adjuvant arthritis in rats. *Int Arch Allergy* 1969; 35:456–467.
11. Pearson CM. Development of arthritis, periarthritis, and periostitis in rats given adjuvants. *Exp Biol Med* 1956;91:95–101.
12. Pearson CM, Wood FD. Studies of arthritis and other lesions induced in rats by the injection of mycobacterial adjuvant. *Am J Pathol* 1963;42: 73–95.
13. Bodziony J, Schwille PO. Subcutaneous cannula in the jugular and femoral vein—a tool for frequent blood sampling and infusions in the rat. *Z Versuchstierk* 1985;27:29–32.
14. Williams AF, Galfre G, Milstein C. Analysis of cell surfaces by xenogeneic myeloma-hybrid antibodies: differentiation antigens of rat lymphocytes. *Cell* 1977;12:663–668.
15. White RAH, Mason DW, Williams AF, Galfre C, Milstein C. T-lymphocyte heterogeneity in the rat: separation of functional subpopulations using a monoclonal antibody. *J Exp Med* 1978;148:664–669.
16. Jefferies WA, Green JR, Williams AF. Authentic T helper CD4 (W3/25) antigen on rat peritoneal macrophages. *J Exp Med* 1985;162:117–127.
17. Mason DW, Williams AF. The kinetics of antibody binding to membrane antigens in solution and at the cell surface. *Biochem J* 1980;187:1–20.
18. Bosslet K, Lüben G, Schwarz A, et al. Immunohistochemical localization and molecular characteristics of three monoclonal antibody-defined epitopes detectable on carcinoembryonic antigen (CEA). *Int J Cancer* 1985; 36:75–84.
19. Schwarz A, Steinsträsser A. A novel approach to Tc-99-labeled monoclonal antibodies. *J Nucl Med* 1987;28:721.
20. Larsson P, Holmdahl R, Dencker L, Klareskog L. In vivo treatment with W3/13 (anti-pan T) but not with OX8 (anti-suppressor/cytotoxic T) monoclonal antibodies impedes the development of adjuvant arthritis in rats. *Immunology* 1985;56:383–391.
21. Kushner I, Somerville JA. Permeability of human synovial membrane to plasma proteins. *Arthritis Rheum* 1971;14:560–570.
22. Rubin RH, Fischmann AJ, Needleman M. Radiolabeled nonspecific, polyclonal human immunoglobulin in the detection of focal inflammation by scintigraphy: comparison with gallium-67-citrate and technetium-99m-labeled albumin. *J Nucl Med* 1989;30:385–389.
23. Calame W, Feitsma HIJ, Ensing GJ, et al. Detection of a local staphylocccal infection in mice with technetium-99m-labeled polyclonal human immunoglobulin. *J Nucl Med* 1991;32:468–474.
24. Fischman AJ, Rubin RH, White JA, et al. Localization of Fc and Fab fragments of nonspecific polyclonal IgG at focal sites of inflammation. *J Nucl Med* 1990;31:1199–1205.
25. Oyen WJG, Claessens RAMJ, Van der Meer JWM, Corstens FHM. Biodistribution and kinetics of radiolabeled proteins in rats with focal inflammation. *J Nucl Med* 1992;33:388–394.
26. Morrel EM, Tompkins RG, Fishman AJ, et al. Autoradiographic method for quantitation of radiolabeled proteins in tissues using indium-111. *J Nucl Med* 1989;30:1538–1545.
27. Fischman AJ, Fucello AJ, Pellegrino-Gensey JL, et al. Effect of carbohydrate modification on the localization of human polyclonal IgG at focal sites of bacterial infection. *J Nucl Med* 1992;33:1378–1382.
28. Breedveld FC, van Kroonenburgh MJPG, Camps JAJ, Feitsma HIJ, Markusse HM, Pauwels EKJ. Imaging of inflammatory arthritis with technetium-99m-labeled IgG. *J Nucl Med* 1989;30:2017–2021.
29. Carrasquillo JA, Bunn PA, Keenan AM, et al. Radioimmunodetection of cutaneous T-cell lymphoma with 111-Indium-labeled T101 monoclonal antibody. *N Engl J Med* 1986;315:673–680.
30. Goldenberg DM, Horowitz JA, Sharkey RM, et al. Targetting, dosimetry, and radioimmunotherapy of B-cell lymphomas with iodine-131-labeled LL2 monoclonal antibody. *J Clin Oncol* 1991;9:548–564.